ELECTRONIC SUPPLEMENTARY MATERIAL FOR THE PAPER

Effect of shallow slip amplification uncertainty on probabilistic tsunami hazard analysis in subduction zones: use of long-term balanced stochastic slip models.

Scala A.[1,2], Lorito S.[2], Romano F.[2], Murphy S.[3], Selva J.[4], Basili R.[2], Babeyko A.[5], Herrero A.[2], Hoechner A.[5], Løvholt F.[6], Maesano F. E.[2], Perfetti P.[4], Tiberti M. M.[2], Tonini R.[2], Volpe M.[2], Davies G.[7], Festa G.[1], Power W.[8], Piatanesi A.[2], Cirella A.[2]

[1] Department of Physics "Ettore Pancini", University of Naples, Italy. Email: scala@fisica.unina.it; antonio.scala@ingv.it;

[2] Istituto Nazionale di Geofisica e Vulcanologia, Sezione di Roma 1, Rome, Italy

[3] Ifremer, Plouzané, France

[4] Istituto Nazionale di Geofisica e Vulcanologia, Sezione di Bologna, Bologna, Italy

[5] GFZ, Postdam, Germany

[6] NGI, Oslo, Norway

[7] Geoscience Australia, Canberra, Australia

[8] GNS Science, Lower Hutt, New Zealand

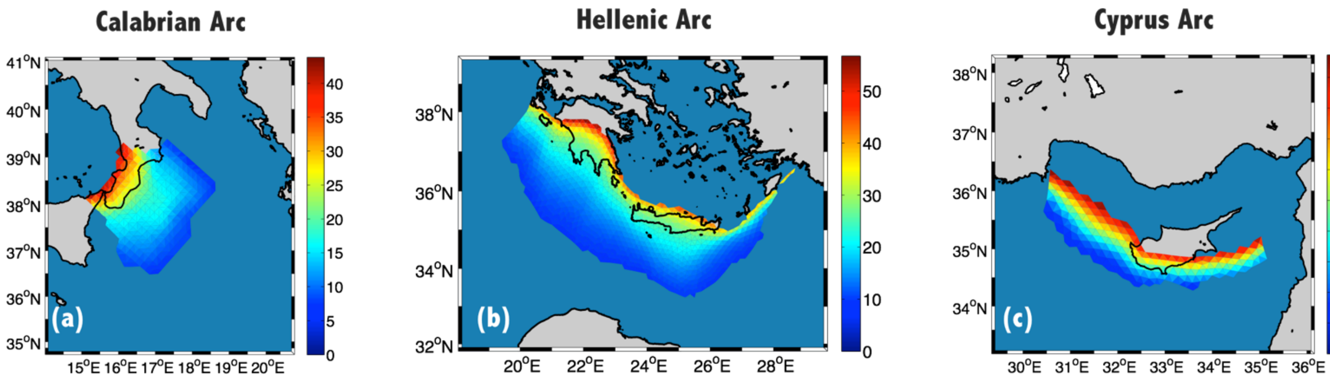

Fig. ESM 1: Meshes of the seismogenic portion of the subduction structures used as case study. Panels **(a)-(b-(c)** refer to the Calabrian, Hellenic and Cyprus arc respectively. The color scale defines the average depth of each cell expressed in km

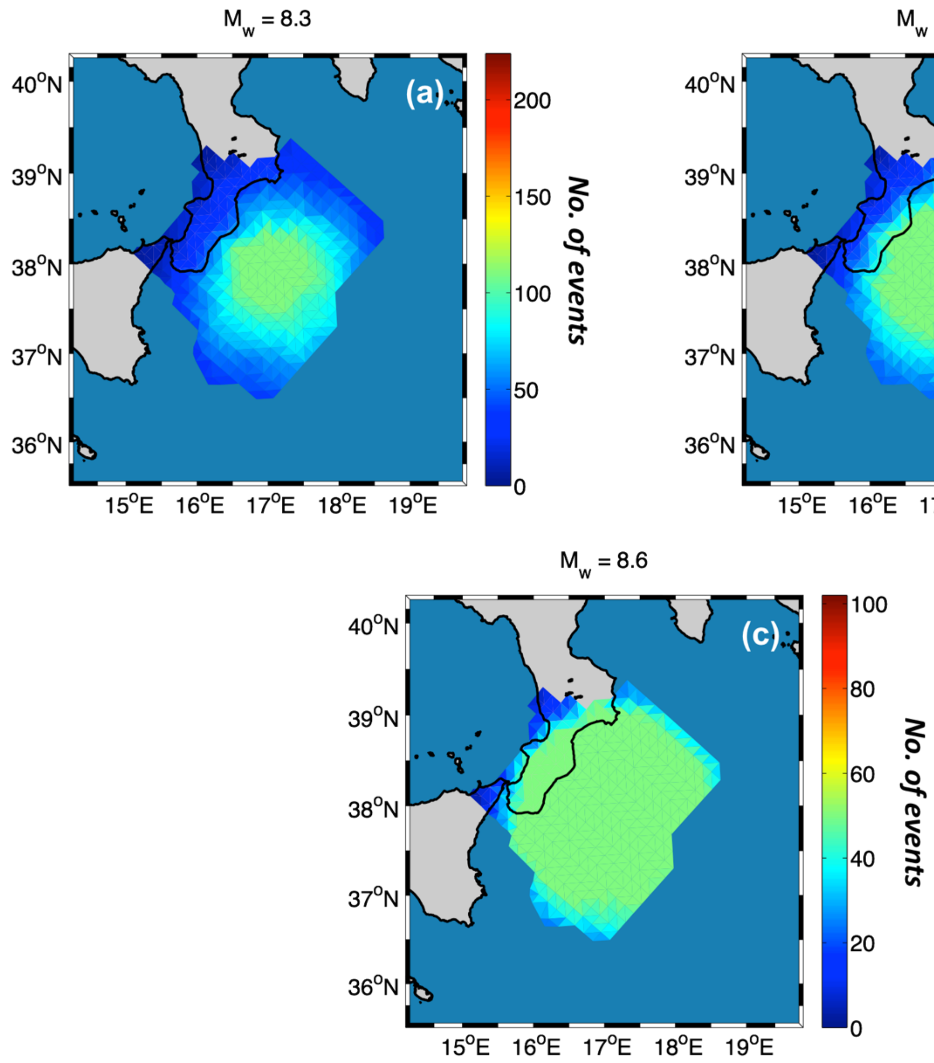

Fig. ESM 2: Number of modelled slip distributions rupturing within each cell on the Calabrian Arc for three different magnitude bins. Panels **(a)-(b)-(c)** refer to $M_w = 8.3; 8.5$ and 8.6 respectively. The panels show that for each magnitude bin the number of events generating slip at the different cells is pretty uniform with a tapering towards the edge.

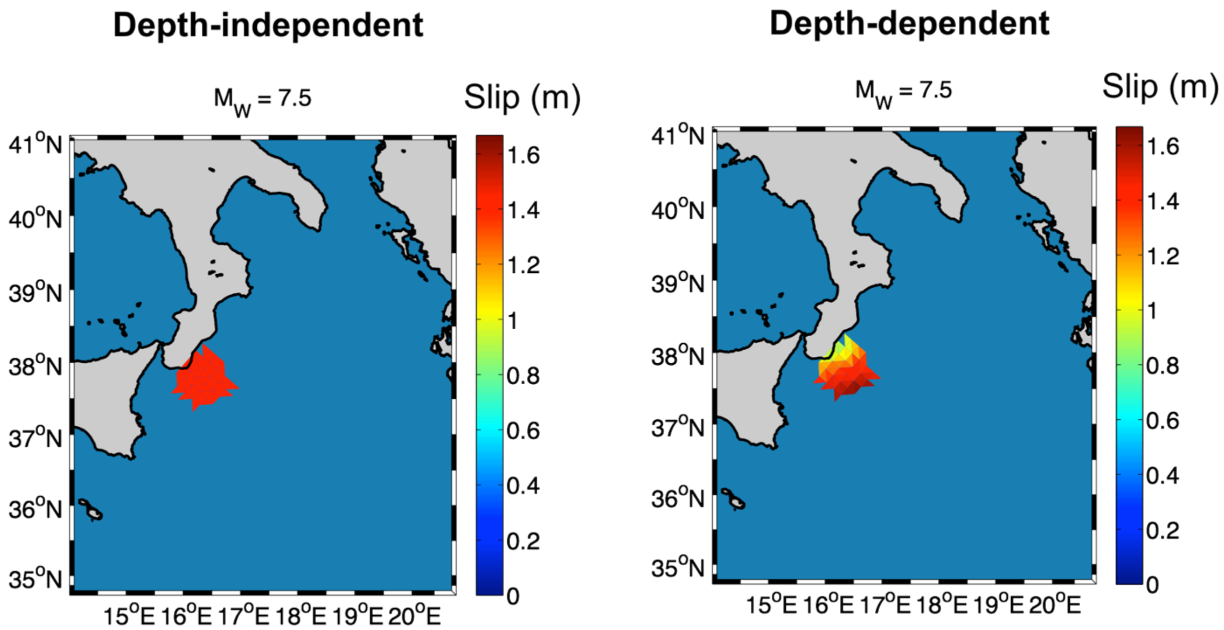

Fig. ESM 3: Illustration of the slip distribution used for small magnitudes. On the left and example of homogeneous slip distribution for the depth-independent set. On the right and example of SWF_n-based slip distribution for the depth dependent set.

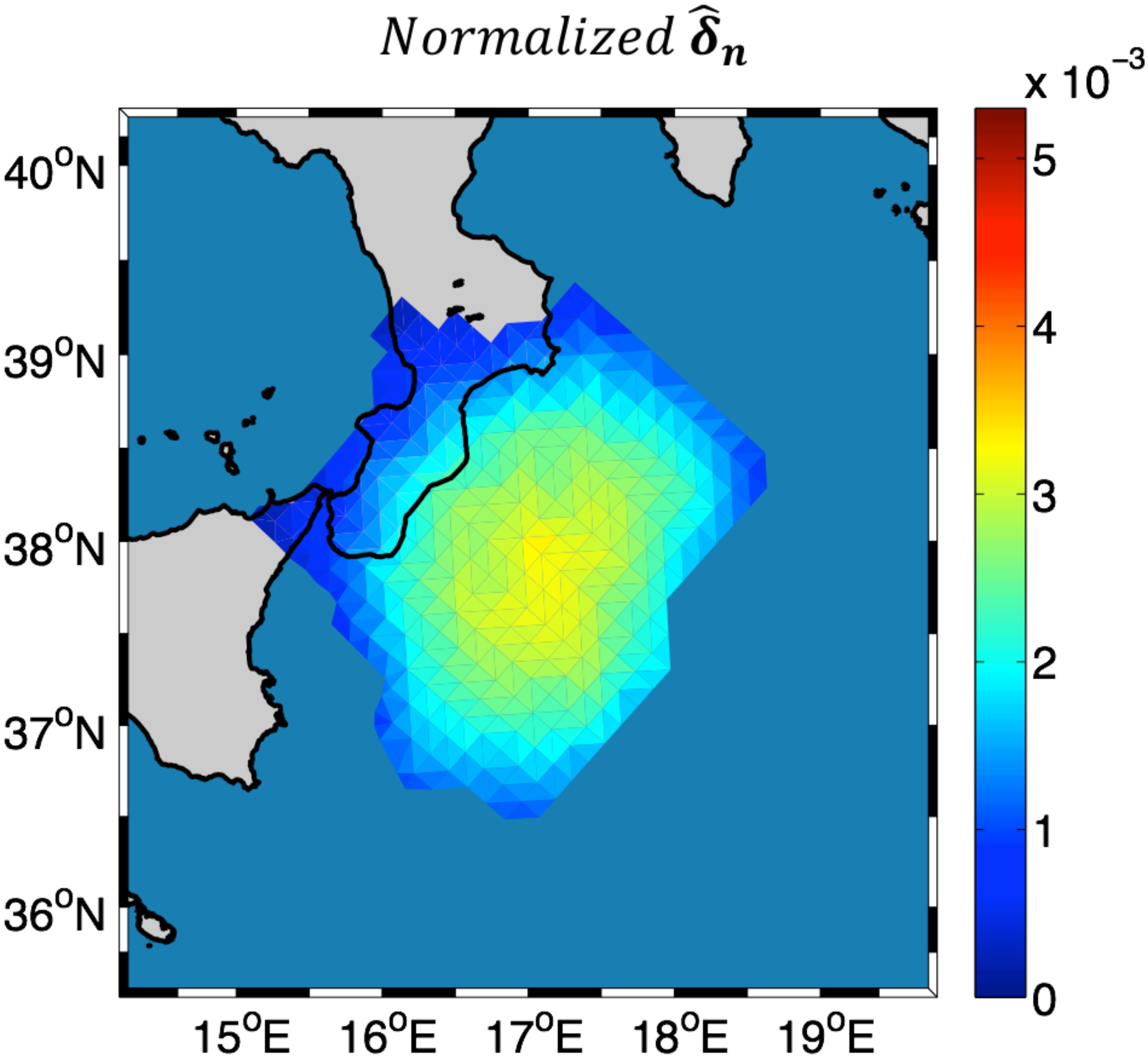

Fig. ESM 4: Estimate of the normalized $\hat{\delta}_n$ for the depth-independent set obtained from the eq. (7) in the main text considering $P(Sl_i|M_w) = 1/N_{M_w}$.

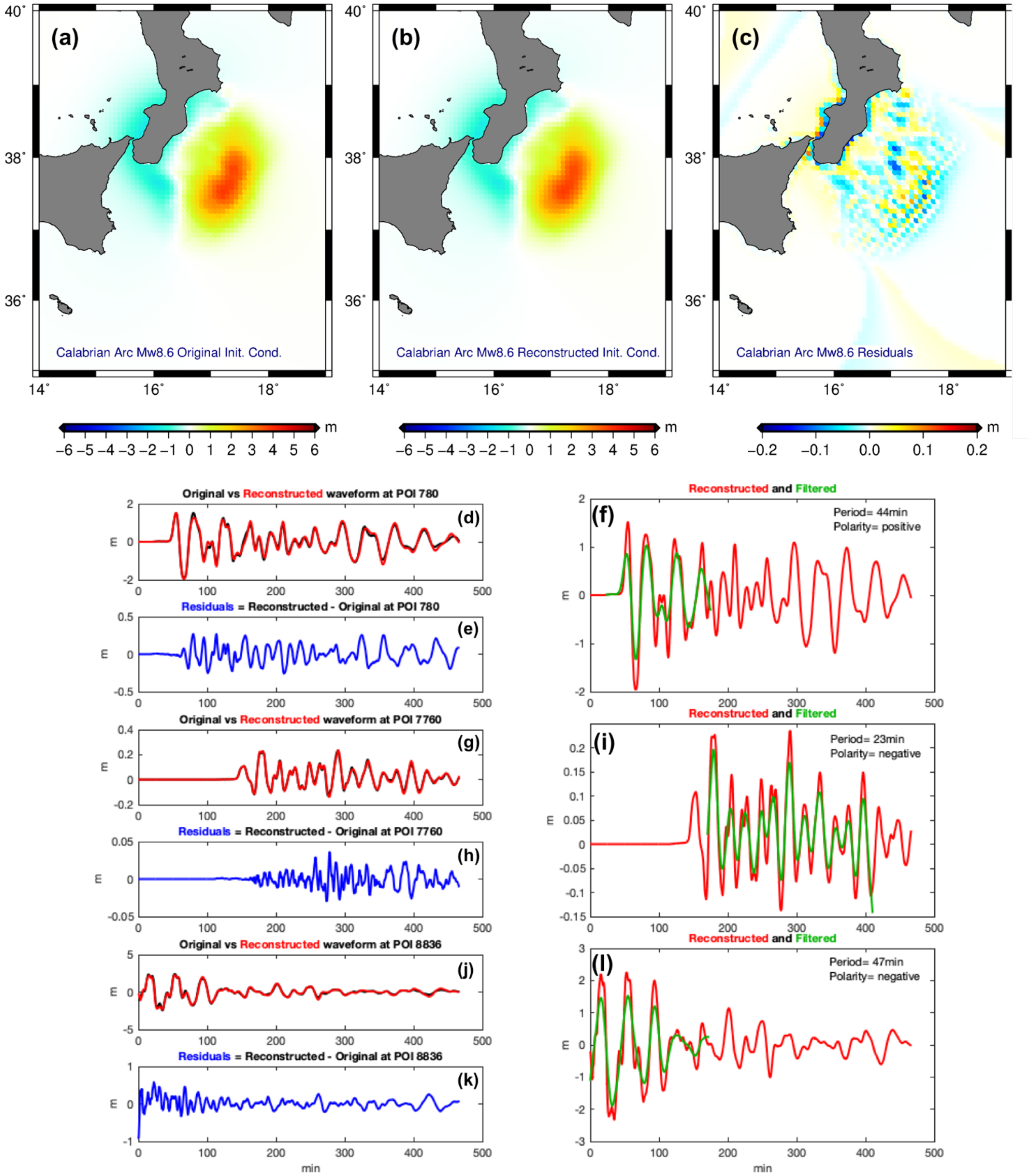

Fig. ESM 5: For a single seismic slip distribution on the Calabrian arc: (a) original initial conditions computed from the slip distribution and (b) their reconstruction through the use of a linear combination of Gaussian elementary displacements. (c) Map of the residual between the original and the reconstructed initial conditions. Relatively to the same slip distribution: (d-g-j) the original and reconstructed mareograms, (e-h-k) the residuals between the two mareograms, and (f-i-l) the filtered mareograms overlapped to the reconstructed ones are plotted for three POIs located on the Peloponnesus, Cyprus and Calabrian coast respectively

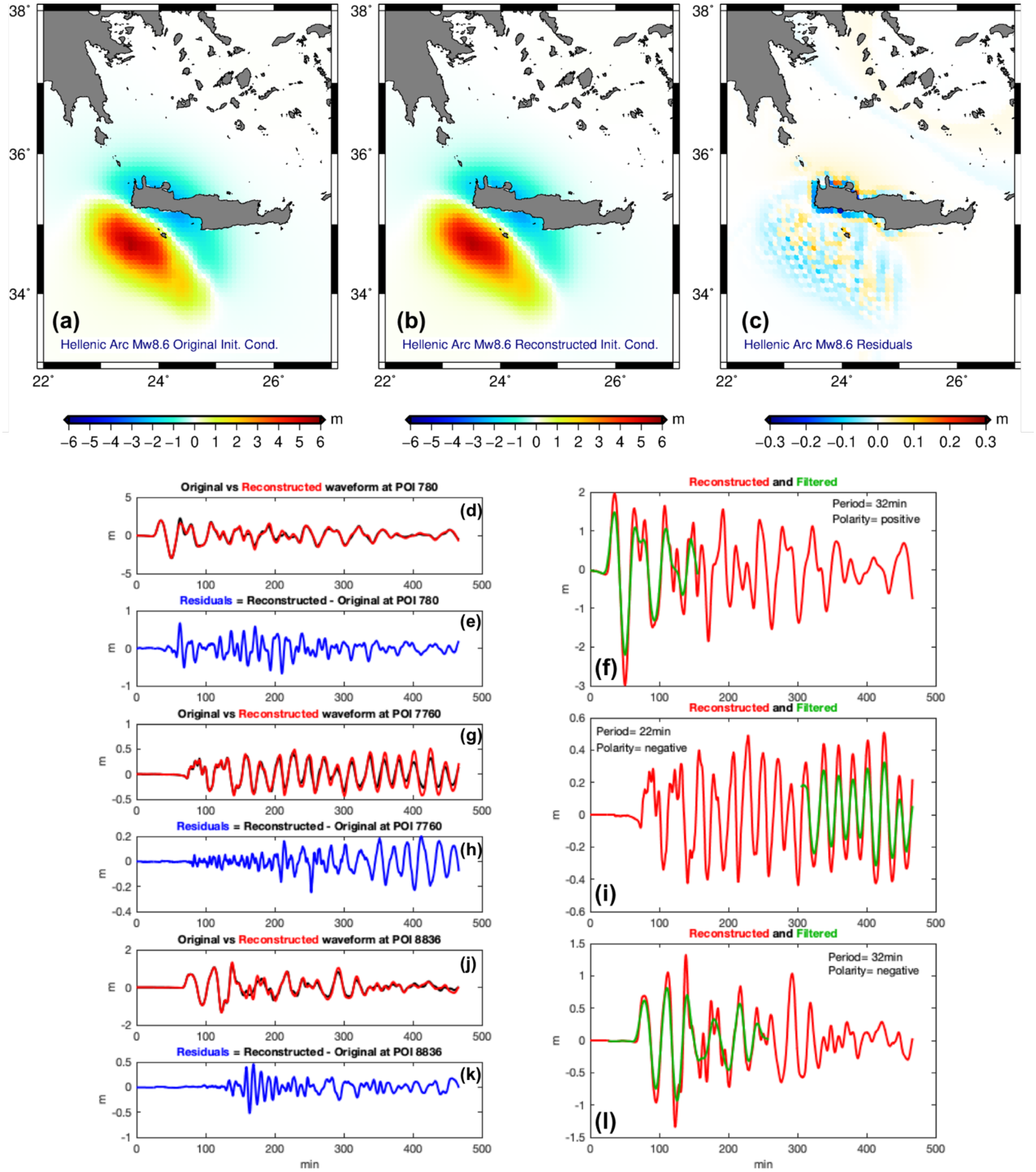

Fig. ESM 6: For a single seismic slip distribution on the Hellenic arc: (a) original initial conditions computed from the slip distribution and (b) their reconstruction through the use of a linear combination of Gaussian elementary displacements. (c) Map of the residual between the original and the reconstructed initial conditions. Relatively to the same slip distribution: (d-g-j) the original and reconstructed mareograms, (e-h-k) the residuals between the two mareograms, and (f-i-l) the filtered mareograms overlapped to the reconstructed ones are plotted for three POIs located on the Peloponnesus, Cyprus and Calabrian coast respectively